Rapid Separation and Quantitative Analysis of Peptides Using a New Nanoelectrospray–Differential Mobility Spectrometer–Mass Spectrometer System

ARTICLE *in* ANALYTICAL CHEMISTRY · SEPTEMBER 2006

Impact Factor: 5.64 · DOI: 10.1021/ac060003f · Source: PubMed

4 AUTHORS, INCLUDING:

Daren S Levin
GlaxoSmithKline plc.
5 PUBLICATIONS **146** CITATIONS
SEE PROFILE

Erkinjon G. Nazarov
Draper Laboratory
93 PUBLICATIONS **2,255** CITATIONS
SEE PROFILE

Anal. Chem. **2006,** *78,* 96−106

Characterization of Gas-Phase Molecular Interactions on Differential Mobility Ion Behavior Utilizing an Electrospray Ionization-Differential Mobility-Mass Spectrometer System

Daren S. Levin,*,† Paul Vouros,† Raanan A. Miller,‡ Erkinjon G. Nazarov,‡ and James C. Morris‡

Department of Chemistry and Chemical Biology and the Barnett Institute of Chemical and Biological Analysis, Northeastern University, Boston, Massachusetts 02115, and Sionex Corporation, 8-A Preston Court, Bedford, Massachusetts 01730

Differential mobility spectrometry (DMS) is a rapidly advancing technology for gas-phase ion separation. The interfacing of DMS with mass spectrometry (MS) offers potential advantages over the use of mass spectrometry alone. Such advantages include improvements to mass spectral signal/noise ratios, orthogonal/complementary ion separation to mass spectrometry, enhanced ion and complexation structural analysis, and potential for rapid analyte quantitation. The introduction of a new ESI-DMS−MS system and its utilization to aid in the understanding of DMS separation theory is described. A current contribution to DMS separation theory is one of an association/dissociation process between ions/molecules in the gas phase during the differential mobility separation. A model study was designed to investigate the molecular dynamics and chemical factors influencing the theorized association/dissociation process, and the mechanisms by which these gas-phase interactions affect an ion's DM behavior. Five piperidine analogues were selected as model analytes, and three alcohol drift gas dopants/modifiers were used to interrogate the analyte ions in the gas phase. Two proposed DMS separation mechanisms, introduced as Core and Façade, corresponding to strong and weak attractions between ions/molecules in the gas phase, are detailed. The proposed mechanisms provide explanation for the observed changes in analyte separation by the various drift gas modifiers. Molecular modeling of the proposed mechanisms provides supportive data and demonstrates the potential for predictive optimization of analyte separation based on drift gas modifier effects.

Differential mobility spectrometry (DMS),[1] also referred to as high-field asymmetric waveform ion mobility spectrometry (FAIMS),[2] and field ion spectrometry[3] is a rapidly advancing technology for gas-phase ion separation. DMS has the potential to emerge as a major stand-alone separation science such as LC or GC. Many researchers have focused on interfacing DMS to mass spectrometry due to its atmospheric pressure, gas-phase, continuous, ion separation capabilities, and the detection specificity offered by mass spectrometry. By interfacing DMS to mass spectrometry, researchers have demonstrated benefits in numerous areas of analysis, including proteomics, peptide/protein conformation, pharmacokinetic, and metabolism analysis.[4−8] In addition to pharmaceutical/biotech applications, DMS has already been incorporated into products designed for trace-level explosives detection as well as petroleum monitoring.[4,9,10]

DMS is related to, but is fundamentally different from conventional time-of-flight ion mobility spectrometry. In conventional ion mobility spectrometry, ion identification is related to effective ion cross section, resulting in differences in flight times. In DMS, ion identification is related to changes in effective cross section based on the propensity of the ion to cluster/decluster, resulting in differences in applied compensation voltage values. In DMS, an ion's mobility does not maintain the same proportionality to the electric field strength when under the influence of a low electric field compared to a high electric field.[10,11] In this manner, the DMS sensor acts as a tunable ion filter, where varying the applied waveform (Rf) and compensation voltages (Vc), allows for selective ion transmission through the sensor.

In DMS, ions are separated at pressures sufficient for the occurrence of collisions between ions and the neutral gas molecules. The smaller the ion, the fewer collisions it will experience as it is pulled through the drift gas. Because of this,

* To whom correspondence should be addressed. Tel: (617) 373-2840. Fax: (617) 373-8795. E-mail: daren.levin@gmail.com.

† Northeastern University.

‡ Sionex Corp.

(1) Buryakov, I. A.; Krylov, E. V.; Nazarov, E. G.; Rasulev, U. Kh. *Int. J. Mass Spectrom. Ion Processes* **1993**, *128*, 143−148.

(2) Purves, R. W.; Guevremont, R.; Day, S.; Pipich, C. W.; Matyjaszcyk, M. S. *Rev. Sci. Instrum.* **1998**, *69*, 4094−4105.

(3) Carnahan, B.; Day, S.; Kouznetsov, V.; Tarassov, A. *Proceedings of the Fourth International Workshop on Ion Mobility*, Cambridge, MA, August 1995.

(4) Guevremont, R. *J. Chromatogr., A* **2004**, 1058, 3−19.

(5) Barnett, D. A.; Ells, B.; Guevremont, R.; Purves, R. W. *J. Am. Soc. Mass Spectrom.* **2002**, *13*, 1282−1291.

(6) Borysik, A. J. H.; Read, P.; Little, D. R.; Bateman, R. H.; Radford, S. E.; Ashcroft, A. E. *Rapid Commun. Mass Spectrom.* **2004**, *18*, 2229−2234.

(7) McCooeye, M.; Ding, L.; Gardner, G. J.; Fraser, C. A.; Lam, J.; Sturgeon, R. E.; Mester, Z. *Anal. Chem.* **2003**, *75*, 2538−2542.

(8) Venne, K.; Bonneil, E.; Eng, K.; Thibault, P. *PharmaGenomics* **2004**, *4*, 30−40.

(9) Eiceman, G. A.; Krylov, E. V.; Krylova, N. S.; Nazarov, E. G.; Miller, R. A. *Anal. Chem.* **2004**, *76*, 4937−4944.

(10) Miller, R. A.; Nazarov, E. G.; Eiceman, G. A.; King, A. T. *Sens. Actuators, A* **2001**, *91*, 307−318.

(11) Miller, R. A.; Eiceman, G. A.; Nazarov, E. G.; King, A. T. *Sens. Actuators, B* **2000**, *67*, 300−306.

10.1021/ac051217k CCC: $33.50
Published on Web 11/24/2005

ion cross-sectional area plays a significant role in its mobility through the drift gas.[10,11] An ion's mobility is not proportional under the influence of a low electric field compared to a high electric field. Miller et al. have described this difference in mobility as being related to clustering/declustering reactions taking place as an ion experiences the high and low electric fields. As described, an ion experiences clustering with neutral molecules in the drift gas during the low-field portion of the waveform, resulting in an increased cross-sectional area. During the high-field portion of the waveform, the cluster is dissociated reducing the ion's effective cross-sectional area.[10]

Within the past five years, much attention in DMS research has focused on understanding the nature of the gas-phase molecular interactions and how they influence ion mobility in the DMS sensor. In 1998, Purves et al. interfaced a FAIMS system to a mass spectrometer to aid in the identification of ions and characterize their FAIMS device. They demonstrated DMS separation of HCO_3^-, CO_3^-, and NO_3^- ions. In doing so, they identified significant DMS separation between the three mentioned ions and two noncovalently bound cluster/dimer ions, $[CO_3 - H - NO_3]^-$ and $[NO_3 - H - NO_3]^-$.[2] Previous work by Krylov et al. demonstrated the DM separation of protonated monomer ketone ions from their corresponding proton-bound dimers.[12] In addition, a study by Krylova et al. demonstrated similar dimer ion separation from their monomer counterparts with various organophosphorus compounds.[13] All of these studies provide substantial evidence that noncovalently bound dimer/cluster ions demonstrate DM behavior different from their monomeric counterparts. This indicates that the cluster/dimer ions were created prior to entering the DMS sensor and were not dissociated back to their monomer counterparts upon entering the asymmetric electric field of the sensor. These studies are significant in that they identify that noncovalently bound cluster ions can survive and be separated by DMS and, in doing so, demonstrate the possibility of altering or controlling an analyte ion's DM behavior through gas-phase molecular clustering interactions. Recently, Eiceman and Krylova et al. have demonstrated changes in DM behavior for various explosives and organophosphorus compounds through the use of various vapor-modified drift gases for which the proposed process is via clustering/declustering interactions between a monomer analyte ion and neutral drift gas modifier/dopant molecule in which the effective cross-sectional area is changed.[9,13]

While previous studies have demonstrated a change in an analyte ion's DM behavior through the use of drift gas modifiers or dopants, a clear model with regard to the underlying interactions between the modifier and analyte, and the mechanism(s) by which those interactions affect DM ion behavior, has not been shown. The present study was designed to investigate the influence of chemical structure, conformational freedom, H-bonding, electrostatic attraction, and steric repulsion on gas-phase molecular interactions and the mechanisms by which they alter DM behavior. For this study, we proposed and investigated mechanisms for some key gas-phase interactions by interrogating selected analytes with specific DMS drift gas modifiers using a novel ESI-DMS−MS system. The analytes and drift gas modifiers were selected, based on their chemical structures, to investigate how their structural properties influence ion clustering/declustering as part of the differential mobility separation process. The compensation voltages for each tested analyte/drift gas modifier condition were determined over a wide range of applied waveform voltage values. In addition, mass spectra were collected at various compensation voltages for each analyte condition to provide insight into ion selection into the mass spectrometer. While our study is limited in scope considering the broad range of possible interactions between analytes and drift gases, we believe the proposed mechanisms are significant for a wide spectrum of DMS applications. Based on the results, two gas-phase interaction mechanisms that detail drift gas modifier effects on analyte ion DM behavior are provided. Molecular modeling calculations with CAChe software enabled an in silico look at the proposed mechanisms. While providing data with strong support of the proposed mechanisms, the molecular modeling data also demonstrated the potential for predicting changes in the DMS separation for various compounds through the use of drift gas modifiers.

EXPERIMENTAL SECTION

Instrumentation. A novel ESI-DMS−MS system was designed encompassing a modified Sionex Corp. microDMx differential mobility sensor (Sionex SDP-1), a Micromass ZQ detector, and a custom-made electrospray source. The ESI source consists of a Valco microconnector union attached to a Newport micromovement plate with *XYZ* directional control. The ESI voltage is applied to the union where a liquid−liquid junction is created between PEEK tubing and a New Objective nanospray tip (part FS360-20-10-N-20). The small size of the DMS sensor module, approximately 3 in. in length, 1 in. in height, and $^1/_4$ in. in width, simplified interfacing to the mass spectrometer inlet. Samples were infused into the electrospray source via a Harvard syringe pump at a flow of 1.25 μL/min. Sample analysis was performed in positive mode electrospray at a capillary voltage of 3.0 KV. A cone voltage of 12 V was applied to the inlet cone of the mass spectrometer. The source temperature for the mass spectrometer was set to 40 °C. Figure 1 demonstrates the ESI-DMS−MS interface design. As shown in Figure 1, a gas line is introduced into the DMS sensor opposite of the electrospray inlet. This provides an introduction site for the drift gas modifier vapors into the sensor as well as the curtain gas for the electrospray inlet. The two detector plates immediately downstream from the separation electrodes provide an ion signal for both positive and negative ions. For our system, a hole was introduced into one of the detector plates to allow for ion transmission into the mass spectrometer. Despite the hole, an ion signal was still generated by the detector plate. The detector plates are biased +5 and − 5 V depending on the ion signal polarity desired. For our system, the positive ion detector plate was assigned to the detector plate with the hole. The vacuum generated by the mass spectrometer provided the gas flow (measured at ~1 L/min) through the sensor and into the mass spectrometer. The gas line opposite the sensor inlet had a constant flow of ultra-high-purity nitrogen at ~0.7 L/min (with or without the addition of modifier). The drift gas modifiers were introduced at a concentration of ~150 ppm of the total gas flow through the sensor. The design and operational details of the Sionex Corp. differential mobility sensors have been

(12) Krylov, E.; Nazarov, E. G.; Miller, R. A.; Tadjikov, B.; Eiceman, G. A. *J. Phys. Chem. A* **2002**, *106*, 5437−5444.
(13) Krylova, N.; Krylov, E.; Eiceman, G. A.; Stone, J. A. *J. Phys. Chem.* **2003**, *107*, 3648−3654.

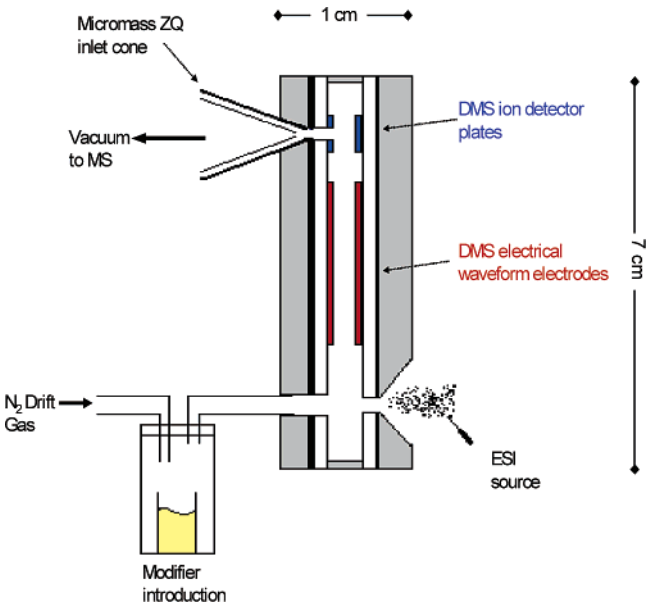

Figure 1. Schematic of ESI-DMS−MS system with approximate dimensions of DMS sensor.

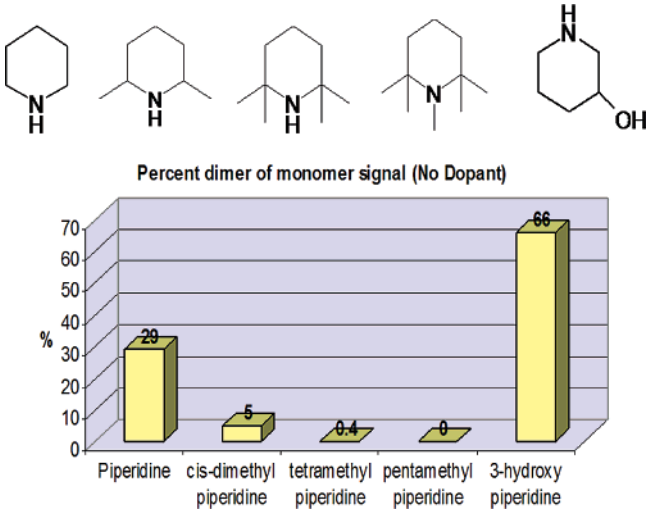

Figure 2. Percentage of mass spectra generated dimer ion signal to monomer ion signal for each analyte with no drift gas modifier and DMS turned off (no separation taking place).

described previously.[9,11,12] For this study, the sensor was operated at ambient laboratory temperature.

Materials and Reagents. Five related compounds, piperidine, *cis*-dimethylpiperidine, tetramethylpiperidine, pentamethylpiperidine, and 3-hydroxypiperidine, were used as test analytes (Sigma-Aldrich Corp., St. Louis, MO). The samples were all prepared at 0.5 mM in a solution of 90% HPLC grade water (Sigma) and 10% HPLC grade methanol (Sigma). 2-Propanol, 2-butanol, and cyclopentanol were tested as the various drift gas modifiers (Sigma). As shown in Figure 2, the drift gas modifier vapors were introduced into the DMS sensor by filling a 5-mL glass vial with the appropriate modifier and placing it within a gas trap style apparatus. Each of the five analytes was tested with and without all three drift gas modifiers.

Molecular Modeling. All molecular modeling experiments were performed with CAChe Worksystem Pro Ver. 6.1.10 software (Fujitsu Corp.) on a Compaq Presario 2100 laptop with an Athlon XP 1800+ processor and 512-mb DDR RAM. Global minimum conformation energy values for all complexes were determined by performing the following experiment: property of, chemical sample conformations (CAChe 5.0 experiments); property, sequence of conformations; using, global minimum search with MM2. Prior to performing the global minimum conformation calculation for each complex, a single chemical sample file containing each component molecule, within proximity, was created. The surface volume values were determined for the minimum energy conformation of each cluster ion.

Procedures. For each sample condition tested, a DMS dispersion plot was generated from the DMS sensor positive ion detector plate signal and by scanning compensation voltages (Vc) from −20 to +5 V for each Rf voltage (asymmetric waveform voltage—reported as the high-field voltage value) ranging from +500 to +1500 V, in 10-V increments. In these experiments, a scan rate of 1.03 s/scan was used for each Vc scan, consisting of 100 steps between −20 and +5 V, enabling an entire dispersion plot to be generated in ~100 s; faster scans can be realized by suitable DMS control. From the dispersion plot data, a DMS spectrum (Vc versus ion signal) can be generated for a given Rf voltage. For any combination Rf and Vc setting from the dispersion plots, a mass spectrum can be collected, providing insight into the ion makeup of a particular Vc point in a DMS spectrum. The DMS spectra are generated from a total ion signal and may contain cluster ions of high mass that are outside of the mass spectrometer's detection range. After the generation of a dispersion plot for each sample condition, Rf and Vc points were selected throughout the plot to collect mass spectra. For each selected Rf and Vc voltage setting, a mass spectrum was collected that averaged 30 s worth of 0.1-s mass scans. Mass spectra were also collected for each sample condition with the DMS turned off, allowing all the ions to enter the mass spectrometer. The combination of dispersion plots and the selected Rf and Vc point mass spectra enabled the construction of accurate Rf versus Vc plots of the maximum ion intensity for all the analyte ions of interest. The Rf versus Vc plots identified the effects of the drift gas modifiers on shifting the analyte ions' Vc for a given Rf. Molecular modeling was used to examine the proposed molecular gas-phase interaction mechanisms taking place.

RESULTS/DISCUSSION

Dimer Ion Formation and Separation. The five substituted piperidine analogues selected for this study were used as model compounds to investigate the effect of structural features on ESI dimer ion formation. It was reasoned that restricting access to the amino group by selective incorporation of methyl groups in its vicinity would have an adverse effect on dimer formation. In contrast, with the addition of a hydrogen-bonding group, as in 3-hydroxypiperidine, it was expected that dimer formation would be enhanced. Figure 2 shows the percentage of dimer ion to monomer ion abundance for each 0.5 mM analyte sample, calculated from their respective mass spectral monomer and dimer ion signals, with the DMS sensor turned off, and using only N_2 as the drift gas. As expected, progressive increase in steric hindrance around the amine resulted in a decrease in dimer abundance. Most notably, the pentamethylpiperidine sample, having the most limited access to the amine, demonstrated no detectable dimer ion. In contrast, a greater than 2-fold increase

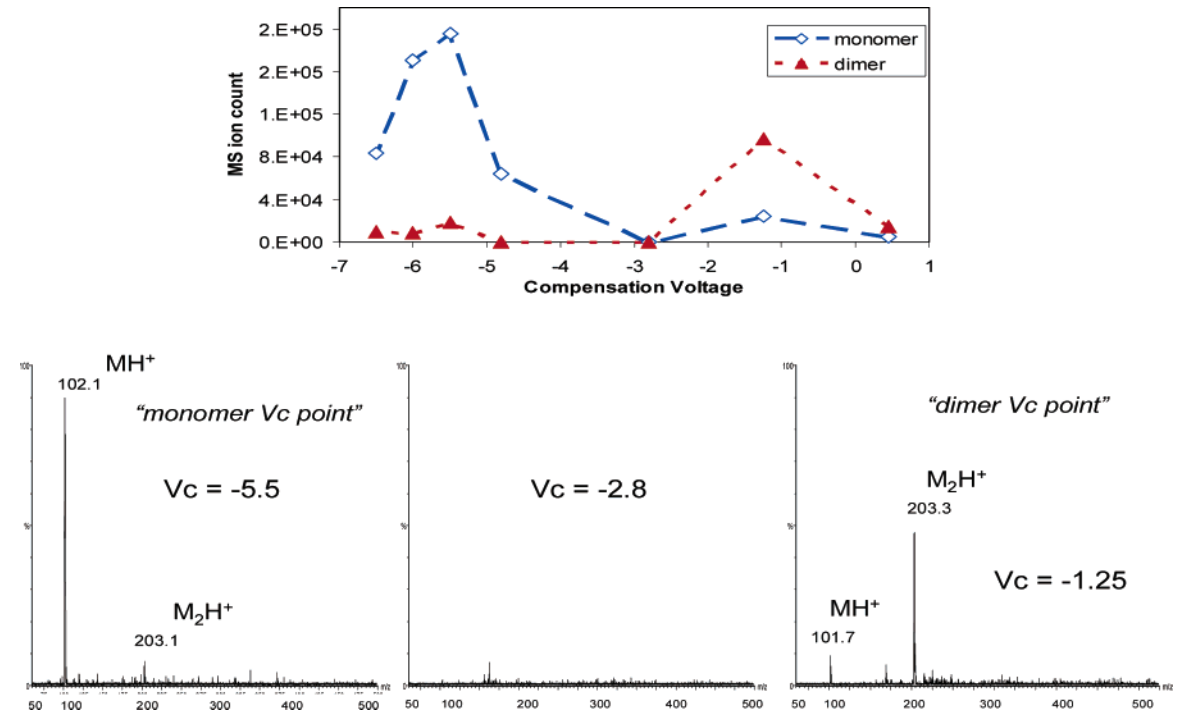

Figure 3. Selected monomer and dimer ion DMS spectra and selected Vc point mass spectra for 0.5 mM sample of 3-hydroxypiperidine with no drift gas modifier (all mass spectra normalized to same ion signal scale).

in dimer signal was observed for 3-hydroxypiperidine compared to piperidine.

For those analytes capable of generating sufficient dimer ion signal, DMS separation between monomer and dimer ions was observed. Figure 3 shows the selected ion DMS spectra for the 3-hydroxypiperidine monomer and dimer ions (top panel), created by plotting their ion signal intensities from mass spectra collected at various compensation voltages (7 different data points), at an Rf voltage of 1000, and without the use of any drift gas modifier. The corresponding mass spectra at the respective DMS peak maximums (Vc point) for the dimer ion of m/z 203 $[2C_5H_{11}NO + H^+]^+$ at Vc = −1.25 V and the monomer ion m/z 102 $[C_5H_{11}NO + H^+]^+$ at Vc = −5.5 V are shown in the lower panel (all spectra normalized to the same ion signal scale). Significantly, no monomer or dimer ion signal was observed at the Vc of −2.8 V, the valley between the two DMS peaks, demonstrating complete separation of the two ion species. However, the mass spectra show the distinct presence of dimer ion along with monomer ion at the −5.5 Vc point. We propose that the presence of dimer ion at the monomer ion Vc point reflects its participation as part of the clustered and declustered states experienced by an ion during the continuously alternating low and high electric fields. In that respect, we refer to the combination of the clustered and declustered states as a quasi "ion equilibrium". This ion equilibrium can be viewed as an association/dissociation process between monomer ion and other molecules in the drift gas forming dimer or other cluster ions as the ions experience the high and low electric fields. During the high-field portion, it is believed that cluster ion dissociation takes place via an increase in the effective temperature of the cluster ion through increased collisions with the drift gas[9,10,13] and possibly via high e-field induced polarization of the cluster ion.

When viewing a Vc point signal as the result of an ion equilibrium, its effective cross-sectional area must take into account the individual cross sections for each participating ion species and their degree of contribution to the equilibrium. It is apparent that the intensity of dimer or cluster ion signal, offered by conventional mass spectrometry, may be significantly underrepresenting the true contribution of the dimer or cluster ions to the equilibrium. Specifically, there is a high probability for declustering of noncovalently bound ions as they pass through the MS inlet. It was therefore necessary to conduct our study at the lowest feasible MS cone voltage setting in order to maintain as much dimer or cluster ion signal as possible.

If the dimer ion is to be considered a true component of the monomer ion Vc point as part of the monomer association/dissociation ion equilibrium, it is necessary to explain its presence in two distinctly separated Vc points for a given Rf voltage. Accordingly, we propose the existence of two modes of dimer formation which may be responsible for the differences in Vc point position as shown in eqs 1 and 2.

$$MH^+ + M \rightarrow MH^{+}\cdots M \quad (1)$$

$$M + M + H^+ \rightarrow M\cdots H^{+}\cdots M \quad (2)$$

Figure 4 shows the proposed molecular conformations of the two different types of protonated 3-hydroxypiperidine dimer ions as determined from CAChe global minimum energy calculation. Figure 4A represents dimer formation between an already protonated analyte ion and a neutral analyte molecule. This type of formation would correlate to the dimer ion that exists as part of the monomer Vc point ion equilibrium. Miller and Krylova et al. described a process of clustering/declustering during differential mobility separation, whereby an analyte ion could cluster with a

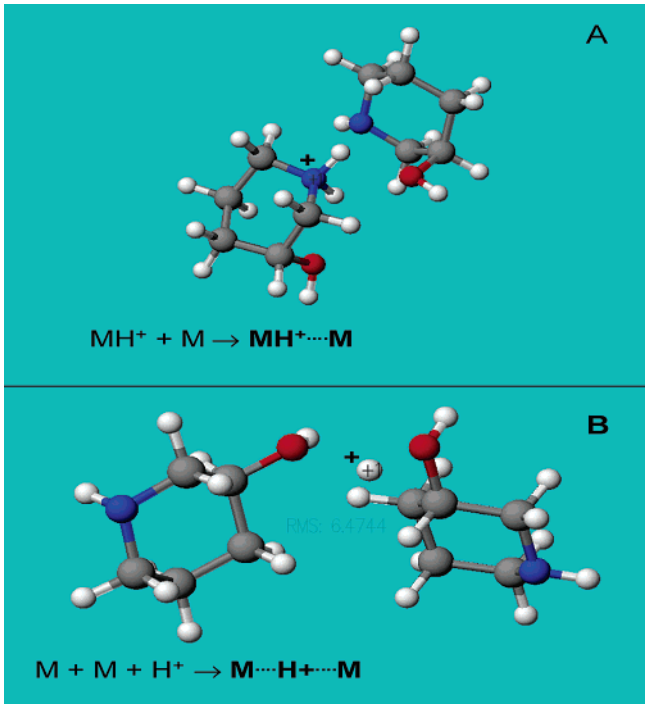

Figure 4. Global minimum energy conformation for two proposed types of dimer ion structures, using 3-hydroxypiperidine as a model analyte. (A) represents dimer ion present in the "monomer Vc point" and is formed between a protonated analyte and a neutral analyte molecule. (B) represents dimer ion present in the "dimer Vc point" and is formed as a shared proton between two neutral analyte molecules.

neutral polar water molecule(s) in the drift gas during the low-field portion of the electrical waveform, effectively increasing the cross-sectional area of the analyte ion. During the high-field portion of the waveform, the cluster would be dissociated, reducing its effective cross-sectional area.[10,13] In accordance with this process, the dimer ion would be continuously forming and dissociating as part of the monomer ion equilibrium, shown in eq 3. In support of this process, Rusyniak et al. demonstrated a

$$MH^+ + M \leftrightarrow MH^{+\cdots}M \qquad (3)$$

change in the time-of-flight ion mobility of the benzene ion by adding neutral benzene molecules into the drift cell, forming postionization benzene dimer ions. In addition, they observed that a difference in the binding energies for the benzene ion and its isomeric fulvene ion, with the neutral benzene molecule, correlated to their degree of dimer associations and effective changes to ion cross section.[14] We propose that, for DMS, the stronger the attraction between the analyte ion and neutral analyte molecule, the longer the dimer ion exists and contributes to the overall cross-sectional area of the ion equilibrium. Alternatively, Figure 4B shows the structure of a 3-hydroxypiperidine dimer ion where a proton is shared by two neutral analyte molecules. This type of dimer is believed to form during the electrospray process in which two neutral analyte molecules compete for the proton addition, resulting in a stable shared proton dimer configuration.

The shared proton dimer model has previously been demonstrated by infrared multiphoton photodissociation spectroscopy for shared proton H_2O dimer ions in the gas phase formed by atmospheric ion spray.[15] In addition, research has demonstrated the existence of both symmetrical (shared proton) and asymmetrical protonated ethanol dimers in solution.[16] We believe this type of symmetrical dimer structure correlates to the dimer ion present in the "dimer ion Vc point" shown in Figure 3 and would represent a structure that may not be as easily dissociated as the dimer structure in Figure 4A, leading to a larger overall cross-sectional area and lower Vc point position. We hypothesize that the dimer structure of Figure 4B does not dissociate under the influence of the high electric field due to its shared proton (symmetrical) structure. Since the proton is shared between two neutral molecules, the primary influence of the electric field is applied to the center of the dimer ion, reducing the potential for dissociation due to e-field-induced ion polarization.

Monomer Ion Equilibrium. Core Mechanism. The evidence presented in the preceding section for the potential existence of two different modes of dimer formation prompted us to investigate next, the role of neutral drift gas modifier molecules in altering analyte monomer ion equilibria via differences in molecular attraction. The addition of modifier may result in a change to the effective cross-sectional area of the monomer ion equilibrium via changes in the participating ion equilibrium species and their degree of contribution. We will refer to this type of effect as a Core interaction mechanism, reflecting a change in an ion equilibrium's core species through the use of a drift gas modifier. Selective changes to analyte ion equilibria, through the use of drift gas modifiers, would reflect the potential for predictive DMS separation control of compounds. Preliminary tests with hydrocarbon gas-phase modifiers, acting as nonpolar controls, and with a molecular size similar to our modifiers used in this study, indicated that the existence of electrostatic attraction between the modifier and analyte ions was vital to altering the DM behavior of our analytes. Accordingly, three different polar gas-phase modifiers—2-propanol, 2-butanol, and cyclopentanol—each providing varying degrees of H-bonding and molecular attraction to the five analytes, were selected for this purpose. Equation 4 depicts

$$MH^+ + \text{modifier} \rightarrow MH^{+\cdots}\text{modifier} \qquad (4)$$

the adduct ion formed between a protonated analyte monomer ion and neutral modifier molecule.

As anticipated, the CAChe global minimum energy calculation for the interaction between the protonated piperidine analyte and the neutral 2-propanol molecule confirmed that the hydroxy group in 2-propanol coordinates directly with the positively charged N in piperidine (data not shown). Figure 5 compares the DMS spectra (generated from the DMS sensor electrometer plate ion signal) for piperidine without (Figure 5A) and with (Figure 5B) the 2-propanol drift gas modifier at an Rf voltage of 1000. The mass spectra in Figure 5A and B were collected at the Rf and Vc settings corresponding to the monomer ion peak maximum ("monomer ion equilibrium Vc point") for each DMS spectrum.

(14) Rusyniak, M.; Ibrahim, Y.; Alsharaeh, E.; Meot-Ner, M.; El-Shall, M. S. *J. Phys. Chem.* **2003**, *107*, 7656−7666.

(15) Asmis, K. R.; Pivonka, N. L.; Santambrogio, G.; Brummer, M.; Kaposta, C.; Neumark, D. M.; Woste, L. *Science* **2003**, *299*, 1375−1377.

(16) Solcá, N.; Dopfer, O. *J. Am. Chem. Soc.* **2004**, *126*, 9520−9521.

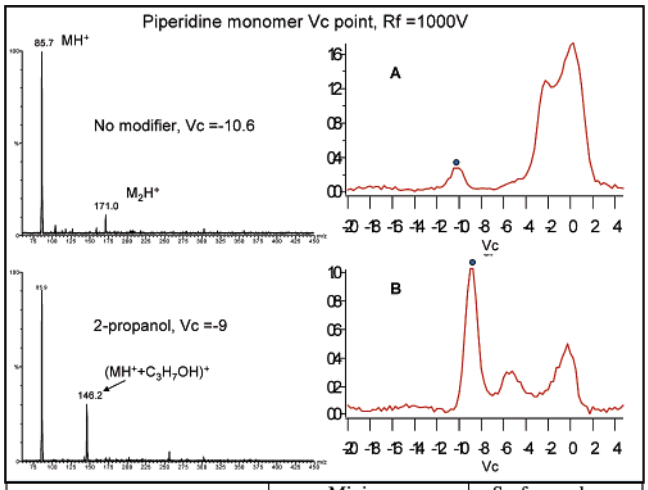

	Minimum conformation energy (kcal/ml)	Surface volume
piperidine(H^+)-piperidine	6.3	7075
piperidine(H^+)-2-propanol	-16.1	6535

Figure 5. DMS spectra for piperidine at an Rf = 1000 V with no modifier (A) and with 2-propanol modifier (B). On the left are the collected mass spectra for the corresponding monomer Vc point (identified by blue circle in DMS spectra). Bottom table shows minimum conformation energy and surface volume values for piperidine dimer and 2-propanol adduct ions determined by molecular modeling.

The *m/z* 86 ion corresponds to the protonated piperidine monomer ion $C_5H_{11}NH^+$, *m/z* 171 is the protonated piperidine dimer ion $[C_5H_{11}N + C_5H_{11}NH^+]^+$, and *m/z* 146 is the piperidine-2-propanol adduct ion $[C_5H_{11}NH^+ + C_3H_7OH]^+$. It is evident that the addition of the 2-propanol modifier produced a new piperidine monomer−modifier adduct ion (*m/z* 146) and resulted in a shift of the monomer Vc point to a lower value, reflecting an increase in the effective ion cross section. Molecular modeling of global minimum conformation energy values were calculated for cluster ions of interest. The energy values are determined by simulating molecular interactions in a vacuum and are not representative of our test environment. However, they do provide comparative data for evaluating differences in the energy of formation for various cluster ions. The global minimum conformation energy values for the piperidine dimer and piperidine-2-propanol adduct ion complexes are shown in the Figure 5 data table. A significant energy difference of 22.4 kcal/mol is observed between the two different complex ions. The lower minimum conformation energy value for the 2-propanol adduct ion complex indicates a greater energy of formation over that of the dimer ion. We hypothesize that the addition of the 2-propanol modifier resulted in an increase in the effective ion cross-sectional area during the clustered portion of the waveform. That is, the difference in energy of formation between the dimer and 2-propanol adduct ions indicate that 2-propanol would foster more clustering with the monomer ion than the neutral piperidine molecule. Similar trends, with regard to shifts in the monomer Vc point and differences in cluster ion global minimum energy values, consistent with the Core mechanism effect demonstrated for piperidine, were observed in the analysis of both dimethylpiperidine and tetramethylpiperidine (data not shown).

As noted earlier, the 3-hydroxypiperidine analyte was selected as a test compound for this study because of its increased propensity for hydrogen bonding and electrostatic interactions on account of the hydroxyl group, and as was shown in Figure 2, it forms the greatest dimer/monomer ion ratio out of all five test compounds. Figure 6 shows its DMS spectra at an Rf of 1000 with no drift gas modifier, with the 2-propanol modifier, and with the 2-butanol modifier, along with their respective mass spectra collected at each monomer Vc point. The introduction of both drift gas modifiers resulted in a shift of the monomer Vc point to a larger Vc value, reflecting a decrease in the effective cross-sectional area of the monomer ion equilibrium. In Figure 6A, we see the *m/z* 102 3-hydroxypiperidine monomer ion as well as the *m/z* 203 singly charged dimer ion $[C_5H_{11}NO + C_5H_{11}NOH^+]^+$. Panels B and C in Figure 6 illustrate the presence of the *m/z* 162 and 176 adduct ions corresponding to the 2-propanol adduct $[C_5H_{11}NOH^+ + C_3H_7OH]^+$ and 2-butanol adduct $[C_5H_{11}NOH^+ + C_4H_9OH]^+$ ions, respectively. Notable in Figure 6 is the consistent dimer to monomer ion ratio observed in all three mass spectra. Unlike that observed for piperidine (Figure 5), the introduction of the drift gas modifiers does not result in a decrease in dimer ion intensity. In the same manner as was done for Figure 3, the selected ion DMS spectra for the monomer, dimer, and 2-propanol adduct ions are displayed in Figure 6B. Demonstrated in the selected ion DMS spectra are the consistent relative intensities, for all three selected ions, across all four data points in the −8 to −12 Vc region of the spectra, supporting the Core mechanism theory. The data table in Figure 6 shows the calculated minimum conformation energy values for the 3-hydroxypiperidine dimer, 3-hydroxypiperidine−2-propanol adduct, and 3-hydroxypiperidine−2-butanol adduct ion complexes. The minimum conformation energy values for the dimer and monomer−alcohol adduct ion complexes are very similar, all within 2.2 kcal/mol of each other, reflecting a nearly equivalent energy of formation for both the dimer and adduct ions. This is in marked contrast to the 22.4 kcal/mol difference seen between the piperidine dimer ion and piperidine−2-propanol adduct ion energy values described earlier. The surface volume values in Figure 6 reflect the volume of space occupied by each ion in their minimum conformation, providing a measure of comparison for cross-sectional area among the three complex ions. As demonstrated by the surface volume values in Figure 6, both modifier−adduct ions have smaller cross-sectional areas than the dimer ion, resulting in a shift of the monomer ion equilibria to larger Vc values. We hypothesize that the reduction in effective cross section is via an overall decrease in ion cross section during the clustered portion of the waveform. That is, the energy of formation values for the dimer and modifier−adduct ions are similar, indicating that the modifiers would result in a comparable degree of clustering as the neutral 3-hydroxypiperidine molecule. Since the individual modifier−adduct ions have smaller cross sections than the dimer ion (surface volume values), a decrease in ion cross section during the clustered portion of the waveform would be expected.

Some aspects of our study design could not be controlled due to the ESI process. In particular, the concentrations of the analyte MH^+ ions and neutral M molecules in the drift gas relative to the

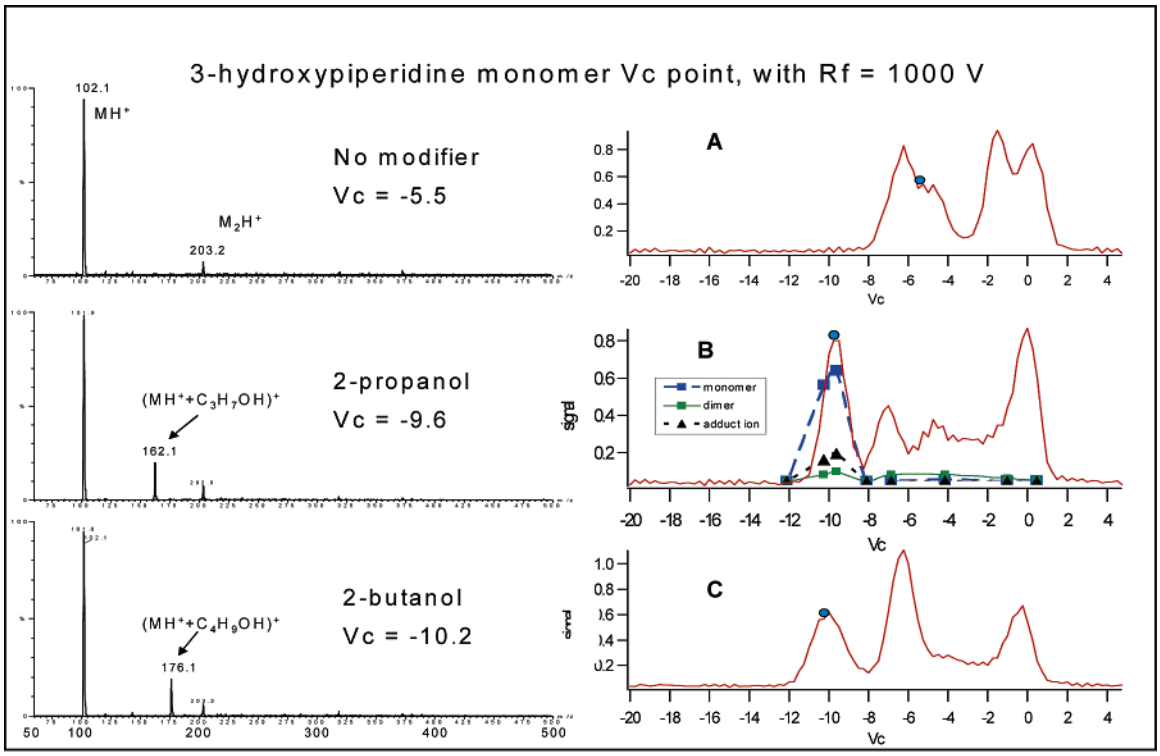

	Minimum conformation energy (kcal/mol)	Surface volume
3hydroxy-piperidine(H^+)-3hydroxy-piperidine	-29.7	7348
3hydroxy-piperidine(H^+)-2-propanol	-31.9	6529
3hydroxy-piperidine(H^+)-2-butanol	-30.2	7178

Figure 6. DMS spectra for 3-hydroxypiperidine at an Rf = 1000 V with no modifier (A), with 2-propanol modifier (as well as overlay of selected ion DMS spectra) (B), and with 2-butanol modifier (C). On the left are the collected mass spectra for the corresponding monomer Vc point (identified by blue circle in DMS spectra). Table below shows molecular modeling determined minimum conformation energy and surface volume values for the 3-hydroxypiperidine dimer, 2-propanol adduct, and 2-butanol adduct ions.

drift gas modifier are unknown and would be expected to play a role in the abundance of formation for a particular cluster ion. However, our use of equimolar samples for all five analytes, as well as equimolar drift gas modifier concentrations, enabled comparisons with respect to differential mobility separation mechanisms and, based on differences in the chemical/physical properties of the analyte and modifier molecules, to be made across all samples.

Monomer Ion Equilibrium. Façade Mechanism. The previous examples have demonstrated the significance of understanding the nature of the gas-phase interactions that govern analyte ion DM behavior. It is clear that each analyte is unique, even within the same class of compounds, and that a given drift gas modification may have opposite effects on shifting Vc point positions for different analytes.

Pentamethylpiperidine was selected as a test analyte for the steric hindrance it provides with regard to spatial access to its protonated nitrogen. Of all five piperidine-related test compounds, pentamethylpiperidine has the most sterically blocked nitrogen atom and demonstrated zero dimer ion signal as shown in Figure 2. Figure 7 shows the DMS spectra and corresponding monomer Vc point mass spectra at an Rf of 1000 for pentamethylpiperidine with; no modifier (A), 2-propanol modifier (D), 2-butanol modifier (C), and cyclopentanol modifier (B). The mass spectra corresponding to the monomer Vc points show the presence of only the m/z 156 pentamethylpiperidine monomer ion, $C_{10}H_{21}NH^+$, for all four conditions. None of the mass spectra demonstrates dimer or drift gas modifier adduct ions. Nevertheless, despite the absence of mass spectrometer signal for dimer or modifier adduct ions at the monomer Vc points, significant shifts of monomer Vc points to larger Vc values occurred with 2-propanol and 2-butanol, as well as a slight Vc shift with cyclopentanol. The monomer Vc point shifts, to larger negative values, indicate a decrease in the effective cross-sectional area for the monomer ion equilibria in the presence of the 2-propanol and 2-butanol drift gas modifiers. This behavior is not consistent with the Core mechanism theory, according to which it would be expected that the effect of a modifier, if any, would result in a shift of monomer Vc point to a lower value. In contrast to the Core mechanism theory, where cluster ions are dissociated primarily during the high-field drift gas collisions and not the low-field portion of the electrical waveform, we suspect that a weak attraction exists between the pentamethylpiperidine monomer ion and the tested drift gas modifiers. This interaction is governed by steric hindrance, which

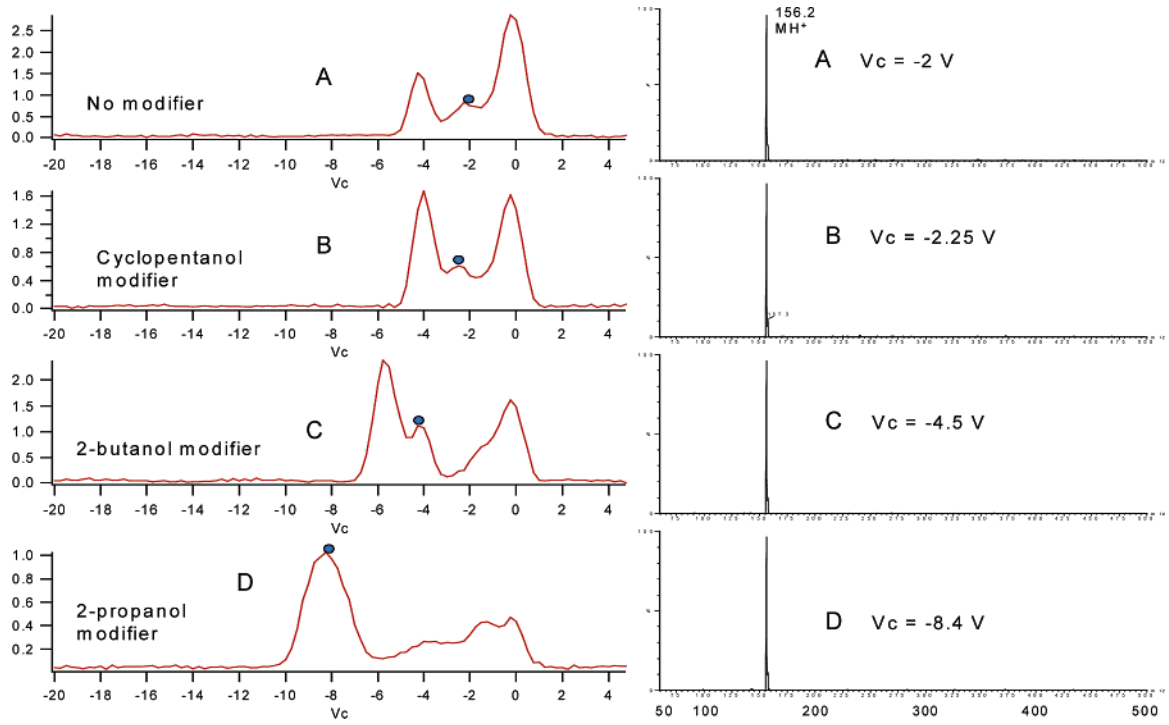

Figure 7. DMS spectra for pentamethylpiperidine at an Rf = 1000 V with no modifier (A), with cyclopentanol modifier (B), with 2-butanol modifier (C), and with 2-propanol modifier (D). On the right are the collected mass spectra for the corresponding monomer Vc point (identified by blue circle in DMS spectra).

causes dissociation of the complex during the drift gas collisions of the low-field portion of the waveform. Notable in Figure 7 is that the smaller the size of the modifier molecule, the greater its effect on decreasing the pentamethylpiperidine effective cross-sectional area, demonstrating that the smaller the modifier, the less steric hindrance and greater attraction to the analyte ion. This hypothesized effect, observed for pentamethylpiperidine, which we will refer to as a Façade interaction mechanism, is one of decreasing an analyte ion's conformational freedom, and in turn reducing the frequency of drift gas collisions with the analyte ion during the low-field portion of the waveform. That is, some of the collisions will strike the weakly held modifier molecule instead of the analyte ion. In comparing the five different analytes, the greater the degree of side-chain branching, the greater the degree of conformational freedom, and potential for a decrease in conformational freedom through the proposed Façade mechanism effect.

While both the Core and Façade mechanisms have been described as two independent gas-phase interaction processes, the reality is that both would probably work synergistically on a sliding scale, dependent on the specific analyte−modifier interaction. The sliding scale model for the two mechanisms can be viewed in relation to the various energetically possible conformations between the two interacting species with some conformations favoring either the Core or Façade mechanisms. Moreover, certain conformations may prevent sufficient attraction between the two molecules, which could negate any effect on differential mobility behavior.

Rf versus Vc Data Plots and Molecular Modeling. Molecular modeling (MM) was used to investigate the proposed Core and Façade mechanisms for the monomer−ion equilibria interactions. Molecular modeling data for global minimum conformation energy and surface volume were collected for each of the test conditions. For analyte conditions with no drift gas modifier, the MM complex data are used to represent the interaction between a single protonated analyte ion and one neutral analyte molecule (dimer ion). For analyte conditions with a drift gas modifier, the MM complex data represent the interaction between a protonated analyte ion and a neutral modifier molecule (analyte−modifier ion). Table 1 summarizes the MM data, providing a measure of comparison for the monomer ion equilibria complex ions, for all

Table 1. CAChe Minimum Conformation Energy and Surface Volume Values for the Proposed Monomer Ion Equilibrium Interactions for All Study Conditions

	min conformation energy (kcal/mol)	surface volume
piperidine(H^+)−piperidine	6.3	7075
piperidine(H^+)−2-propanol	−16.1	6535
piperidine(H^+)−2-butanol	−15.3	6739
piperidine(H^+)−cyclopentanol	−7.2	6949
dimethylpip(H^+)−dimethylpip	9.1	8623
dimethylpip(H^+)−2-propanol	−13.7	7173
dimethylpip(H^+)−2-butanol	−12.9	7644
dimethylpip(H^+)−cyclopentanol	−4.9	7689
tetramethpip(H^+)−tetramethpip	23.1	9823
tetramethpip(H^+)−2-propanol	−6.7	7811
tetramethpip(H^+)−2-butanol	−1.5	8270
tetramethpip(H^+)-cyclopentanol	2.53	8343
pentamethpip(H^+)−pentamethpip	45	10531
pentamethpip(H^+)−2-propanol	10.7	8070
pentamethpip(H^+)−2-butanol	12.3	8565
pentamethpip(H^+)−cyclopentanol	20.2	8576
3hydroxypip(H^+)−3-hydroxypip	−29.7	7348
3hydroxypip(H^+)−2-propanol	−31.9	6529
3hydroxypip(H^+)−2-butanol	−30.2	7178
3hydroxypip(H^+)−cyclopentanol	−22.5	7050

Table 2. Sample (dimethyl-piperidine) and Modifier (2-butanol) Concentration Dependency on Monomer Vc Point Positions at an Rf of 1000V

dimethylpiperidine concn (mM)	monomer Vc point at Rf = 1000			
	no modifier	25 ppm	150 ppm	8000 ppm
0.1	−11	−6.5	−6.8	−14.7
0.5	−10.9	−7.9	−7.6	−15.2
5	−10 to −8.6	−8	−9	−14.8

study conditions. Notable is the correlation between each analyte's dimer ion minimum conformation energy value in Table 2 (6.3, 9.1, 23.1, 45, and −29.7) and the actual MS dimer ion signal intensity percentages shown in Figure 2.

As described previously, the DMS dispersion plots, DMS spectra, and mass spectra for various Rf and Vc settings were used to accurately identify the monomer and dimer ion equilibria Vc point positions for various Rf settings. Based on these data, Rf versus Vc plots were generated for each test compound and drift gas modifier condition. Figure 8 demonstrates the monomer ion equilibria plots for each analyte with and without the drift gas modifiers. A second-order polynomial trend line was calculated from the available Vc data points of each test condition and included in the Figure 8 plots. Notable in Panels B−D in Figure 8 are the comparisons of the Rf versus Vc plots for piperidine, dimethylpiperidine, and tetramethylpiperidine, with and without the 2-propanol drift gas modifier. The use of the 2-propanol modifier resulted in a shift of the monomer Vc point to a greater Vc value for dimethylpiperidine and tetramethylpiperidine but not for piperidine. It is expected that the lack of methyl side chains for piperidine results in lower degree of conformational freedom than for the dimethyl and tetramethyl analytes. This would indicate

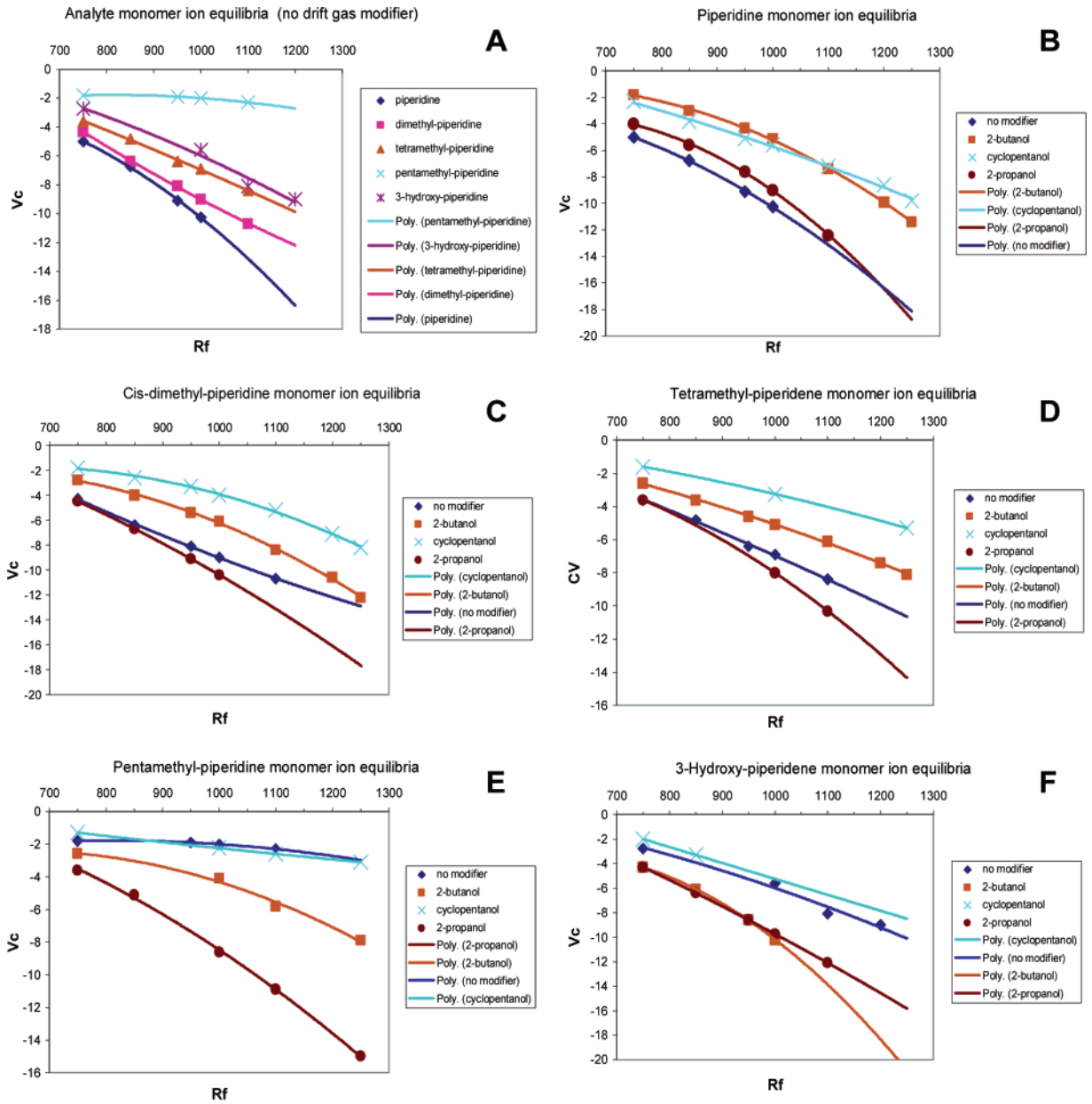

Figure 8. Rf versus Vc plots of the monomer ion equilibria Vc maximUMS for all five analytes with and without the drift gas modifiers. (A) compares all five analytes without any modifier, (B) all piperidine conditions, (C) dimethylpiperidine, (D) tetramethylpiperidine, (E) pentamethylpiperidine, and (F) 3-hydroxypiperidine.

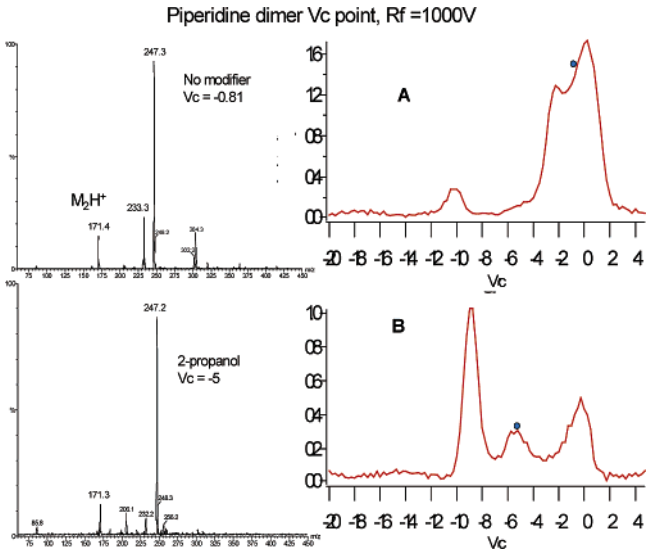

Figure 9. DMS spectra for piperidine at an Rf = 1000 V with no modifier (A) and with 2-propanol modifier (B). On the left are the collected mass spectra for the corresponding dimer Vc point (identified by blue circle in DMS spectra).

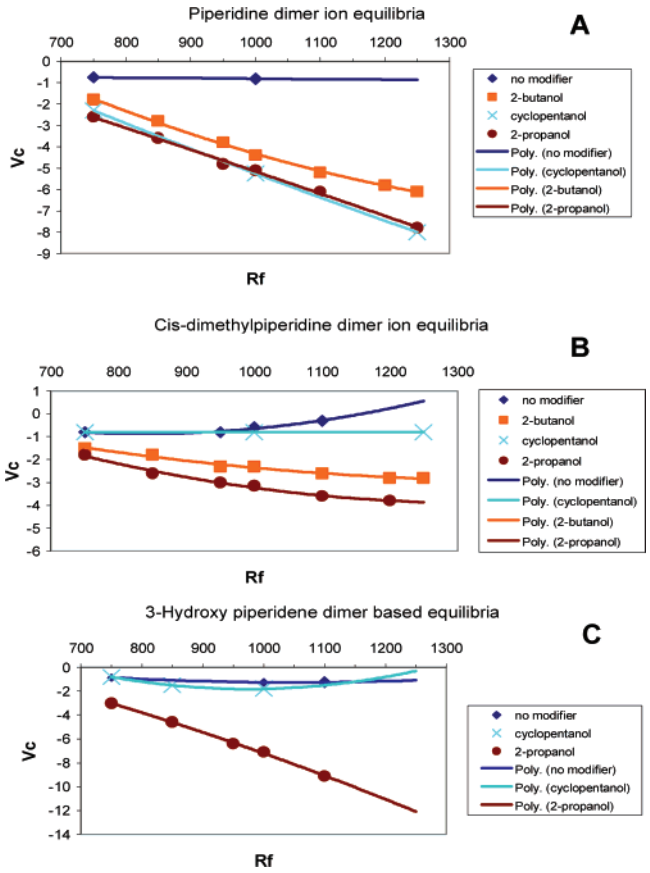

Figure 10. Rf versus Vc plots of the dimer ion equilibria Vc maximums for piperidine (A), dimethylpiperidine (B), and 3-hydroxypiperidine (C) with and without the drift gas modifiers.

that the potential for Façade mechanism to decrease the effective cross-sectional area of the piperidine monomer ion equilibrium is less than for all of the other analytes. Thus, we suggest that the combined effects of the Façade and Core mechanisms provide an overall decrease to the effective cross-sectional area of the monomer ion equilibrium for dimethylpiperidine and tetramethylpiperidine with the 2-propanol modifier. However, the reduced potential for the Façade mechanism effect on the piperidine monomer ion equilibrium results in a more dominant Core mechanism contribution and an increase to the effective cross section.

Dimer Ion Equilibrium. As discussed previously, two mechanisms of dimer ion formation are proposed, to explain the dimer ion presence in both a "dimer ion Vc point" and "monomer ion Vc point". It is presumed that the shared proton dimer structure shown in Figure 4B corresponds to the dimer Vc point. It is proposed that this dimer structure is not easily dissociated in the DMS electric field. Figure 9 shows the DMS spectra, highlighting the dimer Vc point positions, and corresponding mass spectra for piperidine, with and without 2-propanol as a drift gas modifier. The use of the 2-propanol drift gas modifier provides a shift in the dimer Vc point position to a larger Vc, reflecting a decrease in the overall cross-sectional area of the dimer ion equilibrium. The m/z 171 ion is the shared proton piperidine dimer ion $[C_5H_{11}N + H^+ + C_5H_{11}N]^+$. The other ions present in the mass spectra are possibly dimer-based adduct ions contributing to the dimer ion equilibrium or independent ions with DM behavior similar to that of the piperidine dimer ion equilibrium. In Figure 9, with and without the modifier, we observe m/z 233 and 247 ions, corresponding to values equal to (dimer + 62 m/z ion) and (dimer + 76 m/z ion). Adduct ions of the same mass difference from the dimer ion, + 62 (m/z 289) and + 76 (m/z 303), were observed for the dimethylpiperidine sample (dimer = m/z 227) with and without 2-butanol (data not shown). While the identity of the clustered molecules has not been determined, the data in Figure 9 demonstrate a higher degree of clustering for the dimer ion of the "dimer Vc point" compared to the dimer ion of the "monomer Vc point". The proposed shared proton dimer structure may support this, due to the easier steric access to the central proton. For both piperidine and dimethylpiperidine, the addition of the drift gas modifier results in a dimer Vc point shift to a greater Vc and a decrease in the intensity of the + 62 and + 76 cluster ions with respect to the dimer ion.

The underlying interaction mechanism taking place does not stand out. It is possible that a core-type mechanism may be taking place, but the dimer−modifier adduct ions are disassociating prior to detection in the mass spectrometer, or a Façade type interaction may be dominating in which the modifier disrupts the clustering or reduces the conformational freedom of the dimer ion. Regardless of the specific mechanism(s), the only drift gas modifier effect on the DM behavior for all analyte dimer ion equilibria was a shift toward a larger Vc. Panels A−C in Figures 10 show the Rf versus Vc plots for the dimer ion equilibria of piperidine, dimethylpiperidine, and 3-hydroxypiperidine. These three analytes were the only ones capable of generating enough dimer ion signal to detect and track the shifts for the dimer ion equilibria. As shown in Figure 10C, no dimer ion equilibrium was present for the 3-hydroxypiperidine with 2-butanol condition due to lack of MS dimer ion signal.

Concentration Dependency. An experiment was performed to examine the effects of sample and drift gas modifier concentration on the differential mobility behavior of the monomer ion equilibrium. The dimethylpiperidine analyte and the 2-butanol drift gas modifier were tested at various concentrations. Dimethyl-

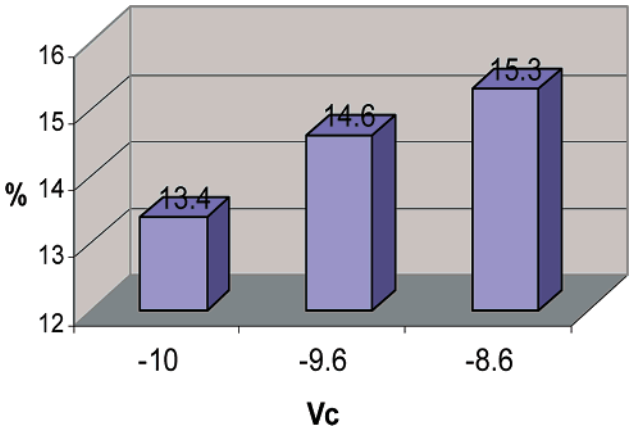

Figure 11. Percent dimer to monomer ion signal at various monomer Vc points, reflecting different ion equilibria cross sections, for the 5 mM dimethylpiperidine sample with no modifier.

piperidine samples at 0.1, 0.5, and 5 mM, were each analyzed with either none, 25, 150, or 8000 ppm of the 2-butanol modifier in the drift gas. The monomer Vc point for each condition was compared at an Rf of 1000 V. The concentration dependency investigation was performed at a date later than all of the previously presented data. During the interim, the ESI-DMS−MS system was disassembled and rebuilt for a laboratory move. A slight but consistent shift in the monomer Vc point position was observed between system setups for the 0.5 mM dimethylpiperidine sample, in the absence and in the presence of the 150 ppm 2-butanol drift gas modifier. Table 2 demonstrates the monomer Vc points for the various sample and modifier concentrations. The 0.1 and 0.5 mM samples demonstrated similar differential mobility behavior for all drift gas modifier conditions. For the 8000 ppm 2-butanol condition, all three sample concentrations experienced the same monomer Vc point shift to a larger Vc compared to the no-modifier condition. This reflects a saturation of the modifier in the drift gas, potentially providing an increased Façade mechanism effect, whereas both the 25 and 150 ppm modifier concentrations foster a dominant Core mechanism effect for the dimethylpiperidine samples. The 5 mM sample demonstrated a broad Vc range (−10 to −8.6) for the maximum monomer ion signal when no modifier was used. Figure 11 demonstrates the percent dimer to monomer ion signal collected from mass spectra at Vc points across that range. A clear correlation between dimer ion contribution to the ion equilibrium and Vc position is demonstrated, substantiating the Core mechanism theory.

CONCLUSION

Differential mobility spectrometry has demonstrated successful gas-phase ion separation at atmospheric pressure for various types of compounds, enabling its use in many areas of chemical/biological analysis. However, in some instances, sufficient separations are not always achievable. Because of this, researchers have begun focusing on ways to improve analyte separation. One of the fundamental ways in which analyte separation can be altered is by changing the pure bulk medium (drift gas) within which the separation is taking place or using modified gas compositions.[9,13,17−19] Recently, Shvartsburg, et al.[18] have demonstrated a first-principles theory for DMS ion behavior in various gas mixtures. Their model focuses mainly on the physical properties of the gas molecules (i.e., mass and cross section) and correlates well to the DM behavior of the monatomic Cs^+ ion in various gas mixtures. The results of our study and the proposed mechanisms suggest that ion−gas collision interactions, based on molecular physical property, alone cannot account for the DM behavior of all analyte ions, particularly polyatomic organic compounds. The potential for an analyte to form dimer/trimer, etc., and cluster ions, driven mainly by the hydrogen-bonding potential, electrostatic attraction, steric repulsion, and energetically favorable conformations of the molecules involved, appears to play a significant role in ion DM behavior. In addition, the conformational freedom and potential for restriction of total conformational space of an analyte ion may have a significant influence on ion DM behavior. In that respect, Krylova and Eiceman et al., and ourselves have demonstrated significant changes in small organic molecule DM behavior through the addition of polar molecule vapors to the drift gas at concentrations ranging from 25 to 9500 ppm of the total drift gas.[9,13] We propose that the Core and Façade mechanisms may be key factors in changing analyte ion DM behavior through the use of drift gas modifications, as well as provide insight into the nature of DMS ion separation. The data generated through molecular modeling of the proposed mechanisms provides support for their use in describing the observed DMS analyte Vc point shifts. In addition to providing support for the proposed mechanisms, the molecular modeling data demonstrated the potential for predicting how an analyte ion would respond to various drift gas modifications. An additional study is currently underway investigating the uses of molecular modeling data to derive comprehensive calculations for predicting analyte Vc point shifts with respect to drift gas modifications. We anticipate future research to expand upon the proposed Core and Façade mechanisms for various compounds and drift gas modifications. In this respect, DMS is still in its infancy with regard to being a separation science. As the knowledge base behind this technology improves, so will its contributions to various types of applications.

Received for review July 8, 2005. Accepted October 28, 2005.

AC051217K

(17) Barnett, D. A.; Ells, B.; Guevremont, R.; Purves, R. W.; Viehland, L. A. *J. Am. Soc. Mass. Spectrom.* **2000**, *11*, 1125−1133.
(18) Shvartsburg, A. A.; Tang, K.; Smith, R. D. *Anal. Chem.* **2004,** 76, 7366−7347.
(19) Barnett, D. A.; Purves, R. W.; Ells, B.; Guevremont, R. *J. Mass Spectrom.* **2000**, *35*, 976−980.